THE JOURNAL OF PHYSICAL CHEMISTRY B

ARTICLE

pubs.acs.org/JPCB

Protein Thermal Denaturation and Matrix Glass Transition in Different Protein−Trehalose−Water Systems

Giuseppe Bellavia,[†] Sergio Giuffrida, Grazia Cottone, Antonio Cupane, and Lorenzo Cordone*

Dipartimento di Fisica, Università di Palermo and CNISM,Via Archirafi 36, I−90123 Palermo, Italy

ABSTRACT: Biopreservation by saccharides is a widely studied issue due to its scientific and technological importance; in particular, ternary amorphous protein−saccharide−water systems are extensively exploited to model the characteristics of the in vivo biopreservation process. We present here a differential scanning calorimetry (DSC) study on amorphous trehalose−water systems with embedded different proteins (myoglobin, lysozyme, BSA, hemoglobin), which differ for charge, surface, and volume properties. In our study, the protein/trehalose molar ratio is kept constant at 1/40, while the water/sugar molar ratio is varied between 2 and 300; results are compared with those obtained for binary trehalose−water systems. DSC upscans offer the possibility of investigating, in the same measurement, the thermodynamic properties of the matrix (glass transition, T_g) and the functional properties of the encapsulated protein (thermal denaturation, T_{den}). At high-to-intermediate hydration, the presence of the proteins increases the glass transition temperature of the encapsulating matrix. The effect mainly depends on size properties, and it can be ascribed to confinement exerted by the protein on the trehalose−water solvent. Conversely, at low hydration, lower T_g values are measured in the presence of proteins: the lack of water promotes sugar−protein interactions, thus weakening the confinement effect and softening the matrix with respect to the binary system. A parallel T_{den} increase is also observed; remarkably, this stabilization can reach ∼70 K at low hydration, a finding potentially of high biotechnological relevance. A linear relationship between T_g and T_{den} is also observed, in line with previous results; this finding suggests that collective water−trehalose interactions, responsible for the glass transition, also influence the protein denaturation.

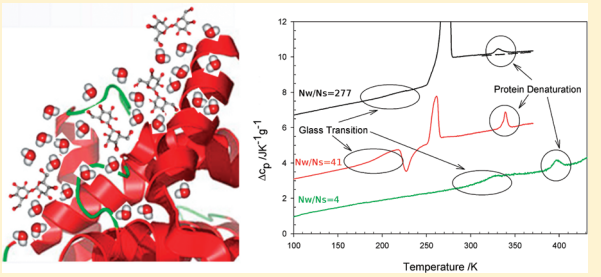

INTRODUCTION

Nature exploits interesting ways to preserve life under adverse environmental conditions such as high temperature and extreme dryness. Anhydrobiosis, i.e., life under conditions of very low hydration, mostly involves a peculiar nonreducing disaccharide, trehalose,[1] which is also known to preserve isolated biostructures such as proteins or membranes. This type of biopreservation is also accomplished, although with lower efficacy, by other saccharides.[2] In view of its interest in both basic science and biotechnological applications in food, drug, and tissue storage, the trehalose peculiarity is presently a matter of study. In this respect, several, often complementary, hypotheses have been proposed.

The first is the water replacement (WR) hypothesis[3] which suggests that, in the dry state, stabilization occurs via the formation of hydrogen bonds (H-B) between the biostructure and the sugar, which substitutes the water in the first hydration shell; this hypothesis is supposed to be at the basis of membrane bioprotection by trehalose.[4−6]

The second hypothesis, i.e., the preferential hydration (PH) hypothesis,[7] suggests that trehalose, rather than directly binding to biomolecules, entraps the residual water at the interface by glass formation, thus preserving the native solvation. This model is an extrapolation to the low hydration state of the suggestions by Timasheff,[8] who reported that in solution trehalose is preferentially excluded from the protein domain; it must be considered, however, that no evidence exists that analogous stabilization mechanisms hold in aqueous solutions and in plasticized low−water systems.[7,9,10]

A third hypothesis, the high viscosity (HV) hypothesis, considers the large viscosity of the host glassy matrix at the basis of bioprotection for low-water systems,[9] since it causes motional inhibition and hindering of the dynamic processes that lead to loss of structure and denaturation.

A further hypothesis by Cesàro and co-workers[11,12] suggests that the peculiarity of trehalose arises from its polymorphism, i.e., its capability to switch between the structurally similar anhydrous form (TRE_α) and dihydrate form (TRE_h): this allows an easy rehydration which leads to a gentle, reversible dehydration−hydration mechanism occurring in nature within the time scale of the main degradation processes.

Another model has been prompted by a number of experimental data, including molecular dynamics (MD) simulations[13] and neutron scattering[14] experiments on binary water−sugar systems. In this model, sugars alter the H-B network in their surroundings with respect to bulk water, with trehalose having

Received: February 11, 2011
Revised: March 23, 2011
Published: April 13, 2011

the largest effect, followed by maltose and sucrose; this suggested that sugar−water interactions are at the basis of the trehalose peculiarity. The same model has been described in terms of host matrix fragility, which, being stronger for trehalose, better slows down the water dynamics and makes trehalose the most effective biopreserver.[15] The characteristic influence of each sugar on the water H-B network in its surroundings is confirmed by differential scanning calorimetry (DSC) data,[16] which showed that the critical water/sugar mole ratio, below which homogeneous glasses are obtained independent of the cooling rate, progressively decreases for trehalose, maltose, and sucrose, being 20, 18, and 15, respectively. The formation of extended H-B networks in saccharide concentrate solutions has also been evidenced with terahertz (THz) spectroscopy. In particular, it has been shown that solutes (sugars, proteins) affect in a peculiar way the fast collective network motions of the solvent well beyond the first solvation layer and that the total THz absorption depends on both the concentration and number of H-B formed with water; again, the effect of trehalose is slightly larger than the other sugars.[17,18]

In line with these observations, and with the reported inhibition of the protein dynamics in trehalose glassy matrixes,[19−22] MD simulations and FTIR measurements on ternary, protein-containing, systems showed that decreasing the sample water content progressively lowers the dynamics of both the matrix and the protein.[23−26] The picture emerging from these data is that the protein is confined within a water-mediated network of hydrogen bonds wherein water molecules, besides connecting sugar molecules to each other, may also connect them to the protein surface. This network "anchors" the protein surface to the matrix, thus coupling the protein internal dynamics to the dynamics of the external matrix.[27,28] This hypothesis, which has been referred to as the "anchorage hypothesis",[29] can be considered as a generalization of the three (WR, PH, and HV) not mutually exclusive models mentioned above. Finally, it should be mentioned that the occurrence of long-range effects in ternary trehalose−water−protein systems has been shown, although on the larger space scale of 1−100 nm, by a small angle X-ray scattering study,[30] which pointed out modifications of the matrix structure triggered by the presence of the protein and modulated by water content.

In the light of these results, one should expect, in ternary protein−water−sugar systems, a marked hydration-dependent effect of the various sugars on parameters related to the structural and dynamical properties of the matrix, e.g., the glass transition temperature, together with a correlated effect on the conformational and/or functional properties of the protein, e.g., the thermal denaturation. In this respect, DSC is a very well suited experimental technique to test the above hypothesis, since DSC upscans enable one to investigate, in a single measurement, the thermodynamic properties of the matrix (glass transition) and the conformational properties of the encapsulated protein (thermal denaturation). In a recent paper,[16] we already studied ternary myoglobin−saccharide−water systems at various hydrations using DSC and we measured the glass transition temperature (T_g) of the matrix and the temperature of thermal denaturation (T_{den}) of the embedded protein; the glass-forming saccharides studied were trehalose, sucrose, maltose, and lactose, with trehalose having the larger effect. Furthermore, a linear correlation between T_g and T_{den} was found, suggesting the existence of a relationship between collective properties that regulate the matrix glass transition, and local properties at the protein/solvent interface that regulate the protein thermal denaturation. However, the observed increase of myoglobin stability against thermal denaturation was rather limited (only ∼10 K). Moreover, the use of a single protein (myoglobin) undermined the generality of the conclusions and prevented one from obtaining detailed information on the type of protein−matrix coupling(s) responsible for the observed effect.

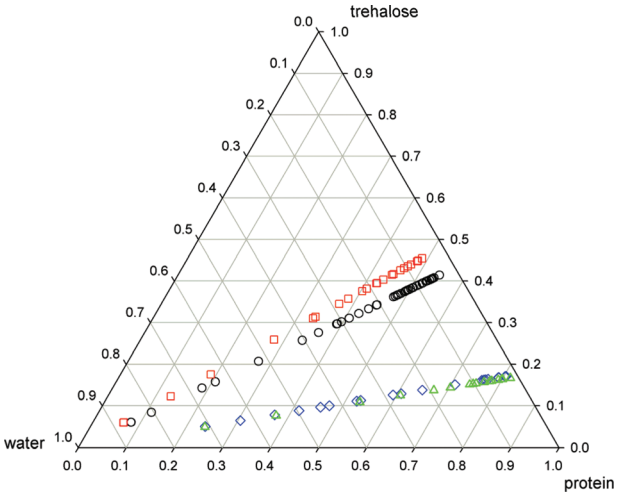

Figure 1. Ternary diagram for the sample composition, expressed as the weight fraction of protein, trehalose, and water: Mb (black circles), LSZ (red squares), BSA (green triangles up), Hb (blue diamonds).

To assess the above points, we present here a DSC study on chicken egg lysozyme (LSZ, positively charged, small size), bovine serum albumin (BSA, negatively charged, large size), and human hemoglobin (Hb, no net charge, large size) embedded in trehalose−water systems, and compare the results with those obtained with myoglobin.[16,31] The aim of the work is to obtain deeper information on the origin of the stabilization enhancement by trehalose, on the role of electrostatic interactions and protein volume (confinement) on the observed quantities (T_g and T_{den}), and ultimately on the physical origin of the protein−matrix coupling in these systems.

MATERIALS AND METHODS

Lyophilized chicken egg white lysozyme (molecular weight, MW, 14.7 kDa, isoelectric point, pI, 11) and bovine serum albumin (MW 66 kDa, pI 4.7), essentially free from fatty acid and globulin, were purchased from Sigma (Sigma, St. Louis, MO) and used without further purification. Trehalose (α-D-glucopyranosyl−α-D-glucopyranoside) from Hayashibara Shoji (Hayashibara Shoji Inc., Okayama, Japan) was used after recrystallization from aqueous solutions. Human adult hemoglobin (MW 64.5 kDa, pI 7.1) was prepared from the blood of a single healthy individual following a standard procedure previously described[32] and stored in liquid nitrogen in the oxygenated form; suitable aliquots were thawed and, after 1 week of freeze−drying, overnight dried at 318 K, thus obtaining a dry methemoglobin powder. Samples were prepared by dissolving proteins (5×10^{-3} M) in a solution containing 2×10^{-1} M trehalose and 2×10^{-2} M phosphate buffer (pH 7 in water), so that a constant trehalose/protein mole ratio (∼40) was achieved. This ratio was chosen, since it allows one to obtain amorphous samples in the whole hydration range without occurrence of either crystallization or

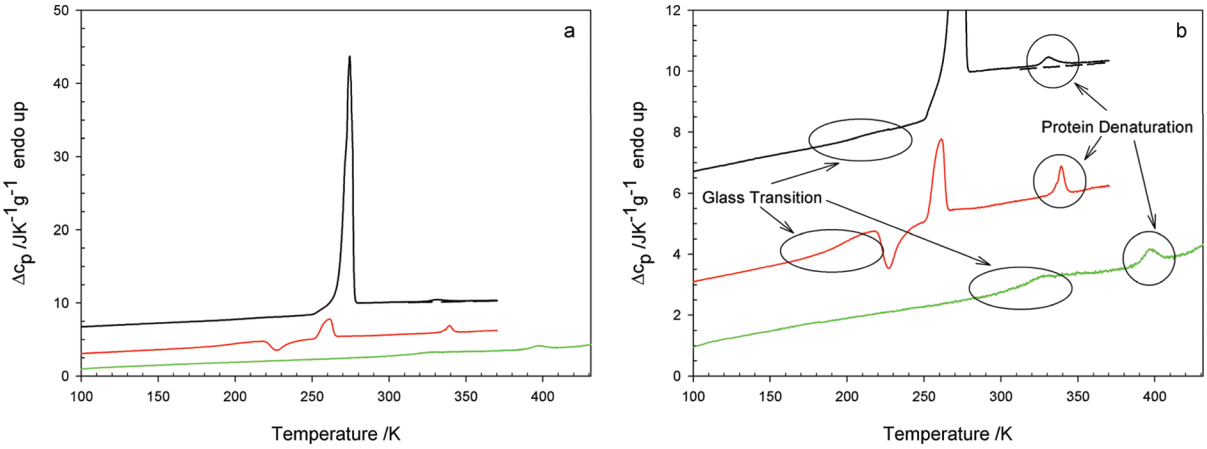

Figure 2. Typical DSC upscans for protein−trehalose−water systems normalized to sample mass. Curves are shifted along the ordinate scale for the sake of clarity. (a) From top to bottom: 277, 41, 4 water/trehalose mole ratio; data refer to a BSA−trehalose−water system. DSC upscans are reported in panel b on an expended scale, to highlight the glass transition and the protein denaturation.

phase separation and approaches *in vivo* anhydrobiotic systems, in which the concentration of embedded biomolecules is quite high with respect to the preserving sugar. Moreover, MD simulations of MbCO embedded in an amorphous plasticized disaccharide system (1 MbCO + ∼250 sugars + ∼600 water) showed that only 40−50 disaccharide molecules are in direct interaction with the protein.[24]

Samples were then gently stirred using a small magnet to ensure full mixing. Aliquots (20 μL) of the above solutions were deposited in aluminum pans for volatile samples of 20 μL maximum volume and ∼23 mg mass, supporting 2 atm pressure. Samples were then blow-dried at 323 K for LSZ and Hb and at 315 K for BSA, until the suitable water/trehalose mole ratio (n_W/n_S) was achieved. The water content was monitored by weighing during blow drying. Aluminum pans were then sealed. Figure 1 shows a ternary plot of the final composition of the samples expressed in weight fraction.

In the case of LSZ, in order to have suitably large protein signals, repeated depositions of solution and blow-drying were performed until reaching water/trehalose ratios spanning from ∼300 to ∼2 and protein content ≥5 mg. At variance, for BSA and Hb, owing to their large molecular weight, a single deposition was sufficient to obtain suitable amounts of protein.

Calorimetric measurements were performed using a Diamond DSC Perkin-Elmer with a Cryofill device using liquid nitrogen as a cold source. Indium was used as a standard to calibrate temperature and heat flow. Heat flow error is 0.05 mW. The temperature program consisted of two identical cycles performed as follows: cooling from 303 to 95 K at 500 K min^{-1}, holding 2 min, then warming at 10 K min^{-1} at least to 373 K, the highest temperature reached depending on the hydration, in order to avoid high pressure. An empty sealed pan was used as a reference. In order to check the baseline stability and to match the aluminum mass contribution, a temperature cycle on a second empty pan was performed after each measurement.

The specific heat was evaluated by subtracting the aluminum heat flow normalized to its mass and then dividing by the scan rate and the sample mass. After subtraction of a suitable cubic polynomial baseline, the T_{den} was determined from the position of the irreversible endothermic peak. The temperature value at the onset of the leap of specific heat, at low temperature, characterized the glass transition temperature (T_g).

RESULTS AND DISCUSSION

Figure 2 shows typical upscan thermograms of protein−trehalose−water systems at various water/trehalose mole ratios. We recall that, in all experiments, the trehalose/protein mole ratio was kept constant at ∼40.

As previously reported for Mb,[16] three different regimes are observed at high, intermediate, and low water content. At high water content, a small ΔC_p (attributed to a glass transition) is followed by a melting peak of water, which overwhelms the thermogram; at intermediate water content, the glass transition is followed by an exothermic crystallization peak followed, in turn, by an endothermic melting peak; at low water content, only the glass transition is observed. All the thermograms show, at high temperatures, an endothermic peak due to the protein denaturation; for LSZ at high water content, the denaturation is partially reversible (data not shown), in agreement with previous results in the literature.[33] In what follows, we shall first discuss the glass transition of the systems, then the protein thermal denaturation, and then their correlation.

Glass Transition. Figure 3 shows the glass transition temperatures of ternary systems containing Mb (panel a, data taken from ref 31), LSZ (panel b), BSA (panel c), and Hb (panel d), as a function of water/trehalose mole ratio; in each panel, the data for the binary trehalose−water system are also reported, for the sake of comparison. As indicated in Figure 3a, the upper region identifies the liquid state, while the lower region is split into two subregions, which respectively identify the ice+mixed systems at high water content, and the glassy states at low water content; the break, which depends on the cooling rate, represents the threshold between glassy and ice+mixed phases. At high hydrations and low temperatures, the systems are inhomogeneous: a large fraction of the water crystallizes (see Figure 2, curve 1), while only a small fraction of the system vitrifies, whose water/trehalose mole ratio corresponds to the so-called maximally freeze−concentrated solute matrix (C_g').[34] The C_g' value is usually obtained by the intercept of the line separating the ice+mixed region from the liquid phase and the curve separating the glassy phase from the liquid phase. Actually, C_g' is related to the maximum number of water molecules that a solute (in this case sugar) molecule can bind; its value delimits the low hydration region in which the whole system undergoes a glass

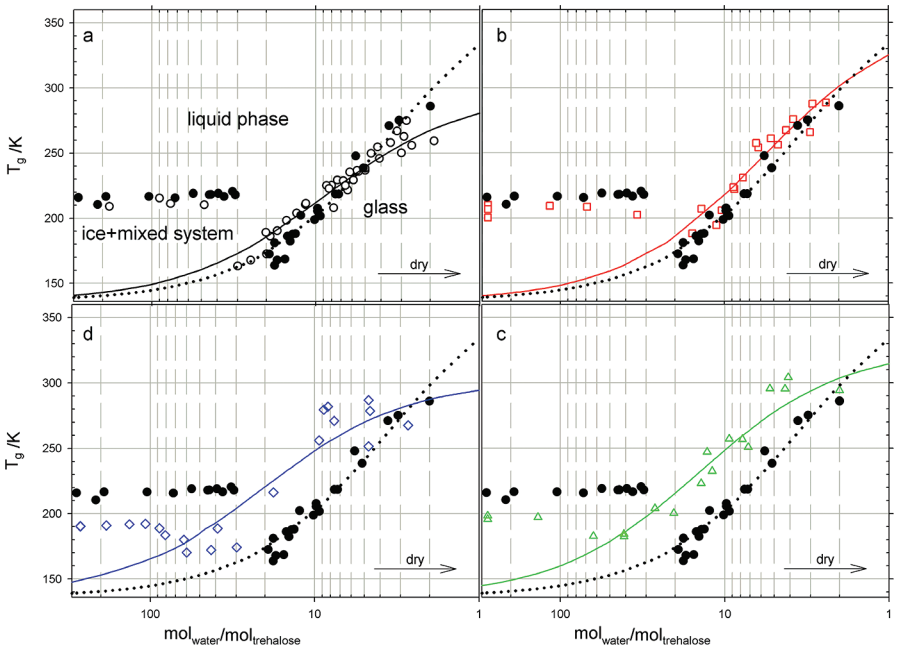

Figure 3. Glass transition temperature as a function of hydration in ternary protein−trehalose−water systems (empty symbols and solid lines) in comparison with the correspondent binary trehalose−water system (full circles and dotted line): Mb (circles), LSZ (squares), BSA (triangles up), Hb (diamonds). Lines are fittings in terms of the G−T formula (eq 1 in the text). (a) Binary system and ternary system with Mb.[31] (b) Binary system and ternary system with LSZ. (c) Binary system and ternary system with BSA. (d) Binary system and ternary system with Hb. As indicated by the arrows, hydration decreases from left to right.

transition, without occurrence of phase separation.[35] At water/sugar ratios higher than C_g', a phase separation takes place, giving a glassy phase with constant composition and constant T_g values (T_g'), while the excess water crystallizes; at water/sugar ratios lower than C_g', the systems are homogeneous and follow the glass−liquid line given by the Gordon−Taylor (G−T) equation.[36] In the plots shown in Figure 3, the G−T equation is obeyed also in a small region at water/sugar ratios higher than C_g', the extension of this region being an increasing function of the cooling rate.

At high water content ($n_W/n_S \geq 5$), all ternary systems investigated show a glass−liquid line shifted toward higher hydration, i.e., an increased T_g at constant water/trehalose molar ratio. The effect is small for smaller proteins (Mb and LSZ) and large for larger proteins (Hb and BSA), marking it as a size effect; at constant protein size, charge effects seem to play a minor role. Moreover, the presence of Mb or LSZ does not sizably alter the C_g' value with respect to the binary trehalose−water systems, while higher values are obtained for the larger size BSA and Hb (Figure 3c,d). Interestingly, the T_g vs n_W/n_S curves relative to the ternary samples are less steep than that relative to the binary system and they cross at n_W/n_S values <5; i.e., while at high hydration ternary systems exhibit T_g values larger than binary systems, they tend to have lower T_g values at low hydration.

The differences observed at high hydration can be explained by considering that all samples have a constant sugar/protein mole ratio and that this makes the (sugar + water)/ protein volume ratio lower for larger protein samples. As pictorially shown in Figure 4, a rough estimate, based on the Voronoi volumes calculated for all the components of the system,[37,38] shows that for Mb and LSZ at a water/trehalose molar ratio of ~10 approximately 50−60% of the total computed volume is occupied by the protein, while the remaining 40−50% is occupied by the water + trehalose solvent; at variance, for Hb and BSA at the same water/trehalose molar ratio, up to 80−90% of the total available volume is occupied by the protein, while only 10−20% is left for the solvent. This implies that the confinement experienced by the water + trehalose fraction is much more severe for Hb and BSA than for Mb and LSZ and explains the observed T_g behavior. On the other hand, the similarity of Mb (uncharged) and LSZ (charged), and of Hb (uncharged) and BSA (charged), suggests that electrostatic effects play a minor role. This interpretation is also compatible with the increase of C_g' values observed for Hb and BSA: in fact, the severe confinement strengthens the network of hydrogen bonds in the system, and widens the hydration region in which the whole system undergoes a glass transition without phase separation.

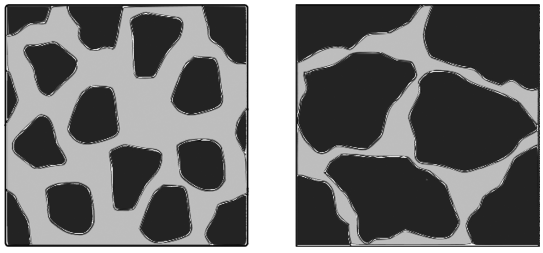

Figure 4. Pictorial sketch of the sample structure to highlight the confinement effect. Dark, protein; gray, water−trehalose matrix. Left panel, Mb and LSZ; right panel, Hb and BSA. For both panels, the dark/gray surface ratio reproduces the (protein)/(water + trehalose) volume ratio in the sample.

At very low hydration, a different mechanism is likely to be at the basis of the T_g decrease: the progressive lacking of water molecules, needed to saturate the sugar H-bond in the matrix,

dx.doi.org/10.1021/jp201378y |J. Phys. Chem. B 2011, 115, 6340–6346

could promote sugar−protein interactions.[24−26] This would cause first the weakening of the confinement effects, then the softening of the sugar−water matrix (which would be coupled to a likely soft system, i.e., the protein close to its melting temperature, through relatively weak H-B), and in turn the reduction of the glass transition temperature of the system.

As for binary water−sugar systems[16] also for ternary systems the T_g values under rapid cooling conditions follow the glass−liquid line even beyond C_g'. The threshold concentration between the glass−liquid line and the constant T_g' line depends on the third component: while the water−trehalose binary system exhibits a break at a water/trehalose molar ratio of ∼20, the break value is at 20−30 in the presence of Mb and LSZ and 60−80 in the presence of BSA and Hb, respectively. The break value indicates the minimal water content, above which homogeneous glassy structure cannot form under our cooling rate, or *vice versa* the maximal water content, below which no ice crystals form under our cooling rate, due to the presence of protein and sugar. Overall, the presence of the protein shifts the break toward higher water contents with respect to the binary system. This stems from the strengthening of the H-B network due to confinement; the different value at which the break appears in the various protein systems again highlights the confinement effect.

To analyze more quantitatively the data in Figure 3, we use the well-known Gordon−Taylor expression[36] extended to ternary systems:

$$T_g = \frac{T_{g,S} + k_{p/s}T_{g,P}\frac{MW_P}{MW_S}\frac{n_P}{n_S} + k_{w/s}T_{g,W}\frac{MW_W}{MW_S}\frac{n_W}{n_S}}{1 + k_{p/s}\frac{MW_P}{MW_S}\frac{n_P}{n_S} + k_{w/s}\frac{MW_W}{MW_S}\frac{n_W}{n_S}} \quad (1)$$

where S stands for sugar, W for water, and P for protein. In our experiments, the protein/sugar mole ratio (n_P/n_S) is kept constant at 1/40; thus, eq 1 depends on n_W/n_S only. In eq 1, $T_{g,S}$, $T_{g,P}$, and $T_{g,W}$ are the glass transition temperatures of the pure components. To avoid fitting ambiguities due to an excessive number of freely adjustable parameters, $T_{g,S}$, $T_{g,P}$, and $T_{g,W}$ values were kept constant at 385, 150, and 136 K, respectively. [The glass transition temperature of pure trehalose (385 K) was taken from ref 39 and refers to calorimetric measurements on anhydrous amorphous trehalose. The glass transition of pure water (136 K) is the classical one reported by Hallbrucker, Mayer, and Johari.[40] We are aware of the fact that the glass transition temperature in water is still debated, with conflicting values reported in the literature and that $T_{g,W}$ = 165 K has been recently reported by Velikov, Borick, and Angell;[41] however, fittings performed by using $T_{g,W}$ = 165 K did not produce any significant difference in our results. The glass transition temperature of proteins at zero hydration (150 K)[42] should not be confused with the so-called "dynamical transition" temperature [43] observed at about 220 K in hydrated protein powders, since this last is absent in dry protein samples. $T_{g,P}$ is more likely related to the dynamical arrest/onset of local side-chain motions (e.g., methyl group or phenylalanine ring dynamics) reported to occur also in dry samples in the temperature interval 100−175 K.[42,44−48] We decided to put $T_{g,P}$ to the average value of 150 K and verified that different choices in the 100−175 K interval did not produce significantly different results.] $k_{W/S}$ and $k_{P/S}$ are nonlinearity parameters gathering the information of our interest on water−trehalose and protein−trehalose interactions, respectively. Note that large values of $k_{W/S}$ indicate a large perturbation of the rigid sugar matrix caused by the addition of water molecules; conversely, small $k_{W/S}$ values correspond to small perturbations and therefore to more rigid water/trehalose matrixes at the same water/trehalose molar ratios. The same argument holds also for $k_{P/S}$: large values of this parameter indicate a large perturbation caused by the protein on the rigidity of the matrix, at low water content.

Table 1. Parameters Obtained from Fittings of T_g vs Water/Trehalose Mole Ratio in Terms of the Generalized G−T Expression for Ternary Systems (eq 1 in the Text)

protein	$k_{W/S}$	$k_{P/S}$
Mb	3.4 ± 0.5	0.58 ± 0.14
LSZ	3.7 ± 0.8	0.1 ± 0.2
BSA	1.8 ± 0.4	0.08 ± 0.04
Hb	1.6 ± 0.5	0.12 ± 0.03

Fittings in terms of eq 1 are reported as solid lines in Figure 3, and are compared to the binary trehalose−water system.[31] Parameter values are reported in Table 1. For all the investigated systems, the effect of protein is to decrease $k_{W/S}$ values with respect to the binary system. As previously noted, the large proteins Hb and BSA have a large effect, while the small proteins Mb and BSA have a small effect. Therefore, the confinement effect already discussed manifests itself in a reduction of parameter $k_{W/S}$, i.e., in a more rigid water/trehalose matrix with a higher T_g value in the presence of proteins, at high hydration. Concerning $k_{P/S}$, very low values (around 0.1) are obtained, indicating that the presence of protein does not alter in a relevant way the rigidity of the sugar/water matrix, even at low hydrations. Interestingly, a larger value of 0.6 is observed for myoglobin and indicates that this protein is more effective in perturbing the encapsulating matrix. The molecular origin of this behavior must reside on the peculiar water and trehalose interactions with the protein surface, although the detailed mechanism is not clear at the present stage: further experimental work will be needed to clarify this point.

Protein Thermal Denaturation. The effect of encapsulation into water/trehalose matrixes on the thermal stability of the investigated proteins can be gathered from Figure 5. In this figure, we report the quantity ΔT_{den} as a function of the water/trehalose mole ratio. $\Delta T_{den}(n_W/n_S) = T_{den}(n_W/n_S) - T_{den}(\infty)$ is the difference between the thermal denaturation temperature of the protein encapsulated in the matrix at a given hydration and that measured in the limit of infinite hydration. These last values were measured to be 349 K for Mb, LSZ, and Hb and 331 K for BSA.

At low hydration, a protein-specific T_{den} increase is observed. As already reported,[16,31] this increase starts at higher water content than for binary protein−water systems and the different behavior can be ascribed to a trehalose−protein competition for binding water molecules. As Figure 5 shows, the T_{den} increase is monotonous for all the proteins and scales in the order Mb ≪ LSZ < BSA ≅ Hb. For Mb, the overall T_{den} variation is much smaller than that for LSZ, BSA, and Hb; in particular, while for Mb the maximal ΔT_{den} value observed is ∼12 K, for BSA and Hb, ΔT_{den} values of about 65 K are obtained already at a water/protein mole ratio of 200. The much lower ΔT_{den} values obtained for Mb can be put in relation with the larger $k_{P/S}$ values

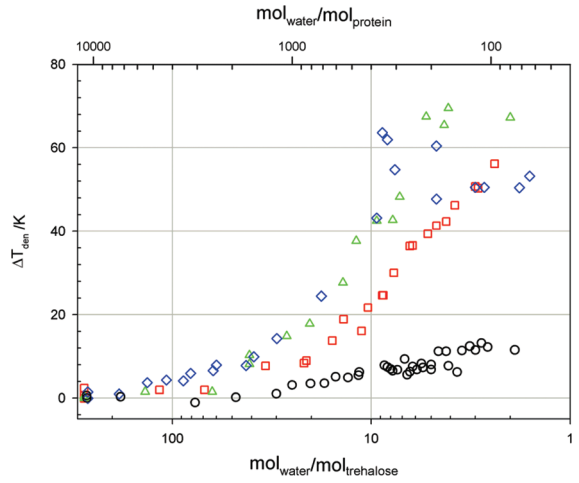

Figure 5. ΔT_{den} as a function of the water/trehalose mole ratio. As indicated by the arrow, hydration decreases from left to right. The water/protein mole ratio is reported in the upper scale. Symbols as in Figure 3.

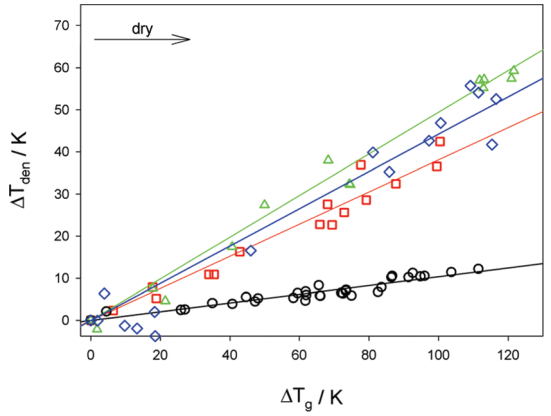

Figure 6. ΔT_{den} as a function of ΔT_g for Mb,[31] LSZ, BSA, and Hb. Symbols as in Figure 3. Lines are linear fittings.

observed for this protein (see Table 1 and discussion in the preceding paragraph) and again indicate that this protein is more effective in perturbing the encapsulating matrix.

At pH 7, Mb is almost uncharged while LSZ is positively charged ($q \sim +8e$) and BSA is negatively charged ($q \sim -15e$); for the latter proteins, the stabilizing effect could therefore be attributed to the electrostatic interactions of the water+trehalose solvent with the protein surface that strengthen the protein−solvent H-B network. Hemoglobin falls outside this scheme, since it shows a huge stabilizing effect while being almost uncharged at pH 7. However, it must be taken into account that for Hb a dimer−tetramer equilibrium is present at room temperature. It may be hypothesized that, at high hydration and at high temperature near the observed T_{den}, a fraction of dimers is present in our Hb samples: we are therefore likely observing essentially the denaturation of hemoglobin dimers. This is supported by the observation that, in the high hydration range, the slopes of the ΔT_{den} vs n_W/n_S curves are identical for Hb and Mb (the fact that the Hb curve is shifted toward higher hydrations may be attributed to the larger exposed protein surface of Hb dimers with respect to Mb). At lower hydration, the increasingly rigid trehalose/water matrix embedding the protein could

Table 2. Parameters Obtained from Linear Fittings of ΔT_{den} vs ΔT_g

protein	α
Mb	0.104 ± 0.005
LSZ	0.38 ± 0.02
BSA	0.49 ± 0.02
Hb	0.44 ± 0.04

shift the dimer−tetramer equilibrium toward the tetrameric conformation and therefore cause the observed relevant T_{den} increase. Further studies on the dimer−tetramer equilibrium of Hb embedded in trehalose/water matrixes will be necessary to test this hypothesis.

In any case, it should be stressed that relevant protection against thermal denaturation (up to $\Delta T_{den} \sim 65$ K) is here reported for proteins (LSZ, BSA, Hb) embedded in trehalose/water matrixes at low hydration. This finding is of obvious technological interest, e.g., in the field of food preservation; further studies aiming at a better characterization of this effect are presently under way.

$T_g - T_{den}$ Correlations. As already mentioned, for our systems, the DSC upscans offer the possibility of investigating in the same measurement the glass transition temperature of the matrix and the thermal stability of the embedded proteins. In order to figure out the possible correlations between the two properties, we report in Figure 6 a ΔT_{den} vs ΔT_g plot. In analogy to the ΔT_{den} definition (see above), ΔT_g is defined as the difference between the glass transition temperature of the matrix at a given hydration and that measured at the highest hydration for which we observe a homogeneous matrix.

As shown in Figure 6, a linear correlation between ΔT_{den} and ΔT_g is observed for all the proteins investigated; the correlation, however, is not universal, since different slopes are observed for different proteins. The linearity can be expressed[34] as $\Delta T_{den} = \alpha \Delta T_g$; α values, reported in Table 2, scale in the order Mb ≪ LSZ < Hb < BSA. The data in Figure 6 confirm what was previously suggested for Mb,[16] i.e., that collective water−trehalose interactions, which determine the glass transition, also influence the protein denaturation. However, the specific protein−matrix interactions, although overwhelmed by confinement effects in determining the glass transition, do influence the denaturation process, thus making the linear correlation specific for each different protein.

CONCLUSIONS

In this work, we simultaneously determined, in the same sample, the glass transition temperature of ternary protein−water−trehalose systems and the protein thermal denaturation as a function of the matrix hydration (water/sugar mole ratio). The study has been extended to several proteins differing in volume, surface, and charge properties, in order to investigate the effects of confinement and electrostatic interactions on the protein−matrix coupling in these systems.

The main results obtained may be summarized as follows:

- At high−to−intermediate hydration the presence of the proteins increases the glass transition temperature of the encapsulating matrix. This effect is larger for high molecular weight proteins and does not depend appreciably on the protein charge; we therefore attribute it to the confinement experienced by the solvent that, due to the constant sugar/

dx.doi.org/10.1021/jp201378y |J. Phys. Chem. B 2011, 115, 6340–6346

protein mole ratio, is much more severe in the case of the Hb and BSA samples than for the Mb and LSZ ones. Large macromolecules could therefore be successfully used in food or pharmaceutical formulations, when increasing the glassy phase range is desirable.[49,50]

- At very low hydration, the lack of water leads to increasing protein−matrix interactions, which weaken the confinement effect; in this case, the sugar matrix would be coupled to the softer protein component through relatively weak H-bonds,[24] depressing the T_g.
- An increase of the protein thermal stability is observed in the whole hydration range; at variance with T_g, the extent of this stabilization depends also on charge effects. It is remarkable that for Hb, LSZ, and BSA the T_{den} increase can reach about 60−70 °C at low hydrations.
- A linear relation between the denaturation temperature of the embedded protein and the glass transition temperature of the matrix is found, specific of each protein. This suggests that collective water−trehalose interactions, responsible for the glass transition, also influence the protein stability, with the stabilization extent depending on the specific protein−matrix interactions.

AUTHOR INFORMATION

Corresponding Author

*E-mail: cordone@fisica.unipa.it.

Present Addresses

[†]UMET - UFR de Physique - BAT P5 UMR CNRS 8207, Université Lille 1, 59655 Villeneuve d'Ascq, France.

ACKNOWLEDGMENT

This work was supported by MIUR (Grant PRIN 2008ZWHZJT Struttura-Dinamica-Funzione di Biomolecole in Sistemi lontani dall'Idealità termodinamica) and local funds (ex-60%).

REFERENCES

(1) Crowe, J. H.; Carpenter, J. F.; Crowe, L. M. *Annu. Rev. Physiol.* **1998**, *60*, 73–103.
(2) Crowe, L. M. *Comp. Biochem. Physiol., A* **2002**, *131*, 505–513.
(3) Carpenter, J. F.; Crowe, J. H. *Biochemistry* **1989**, *28*, 3916–3922.
(4) Sum, A. K.; Faller, R.; de Pablo, J. J. *Biophys. J.* **2003**, *85*, 2830–2844.
(5) Pereira, C.; Lins, R. D.; Chandrasekhar, I.; Freitas, L. C. G.; Hunenberger, P. H. *Biophys. J.* **2004**, *86*, 2273–2285.
(6) Pereira, C.; Hunenberger, P. H. *J. Phys. Chem. B* **2006**, *110*, 15572–15581.
(7) Belton, P. S.; Gil, A. M. *Biopolymers* **1994**, *34*, 957–961.
(8) Timasheff, S. N. *Biochemistry* **2002**, *41*, 13474–13482.
(9) Sampedro, J. G.; Uribe, S. *Mol. Cell. Biochem.* **2004**, *256*, 319–327.
(10) Green, J. L.; Angell, C. A. *J. Phys. Chem.* **1989**, *93*, 2880–2882.
(11) Sussich, F.; Skopec, C.; Brady, J.; Cesàro, A. *Carbohydr. Res.* **2001**, *334*, 165–176.
(12) Cesàro, A. *Nat. Mater.* **2006**, *5*, 593–594.
(13) Lerbret, A.; Bordat, P.; Affouard, F.; Descamps, M.; Migliardo, F. *J. Phys. Chem. B* **2005**, *109*, 11046–11057.
(14) Magazù, S.; Maisano, G.; Migliardo, F.; Mondelli, C. *Biophys. J.* **2004**, *86*, 3241–3249.
(15) Varga, B.; Migliardo, F.; Takacs, E.; Vertessy, B.; Magazù, S.; Telling, M. T. F. *J. Biol. Phys.* **2010**, *36*, 207–220.
(16) Bellavia, G.; Cottone, G.; Giuffrida, S.; Cupane, A.; Cordone, L. *J. Phys. Chem. B* **2009**, *113*, 11543–11549.
(17) Heyden, M.; Bründermann, E.; Heugen, U.; Niehues, G.; Leitner, D. M.; Havenith, M. *J. Am. Chem. Soc.* **2008**, *130*, 5773–5779.
(18) Ebbinghaus, S.; Kim, S. J.; Heyden, M.; Yu, X.; Heugen, U.; Gruebele, M.; Leitner, D. M.; Havenith, M. *Proc. Natl. Acad. Sci. U.S.A.* **2007**, *104*, 20749–20752.
(19) Hagen, J.; Hofrichter, J.; Eaton, W. A. *Science* **1995**, *269*, 959–962.
(20) Gottfried, D. S.; Peterson, E. S.; Sheikh, A. G.; Wang, J.; Yang, M.; Friedman, J. M. *J. Phys. Chem.* **1996**, *100*, 12034–12042.
(21) Cordone, L.; Ferrand, M.; Vitrano, E.; Zaccai, G. *Biophys. J.* **1999**, *76*, 1043–1047.
(22) Cordone, L.; Cottone, G.; Giuffrida, S.; Librizzi, F. *Chem. Phys.* **2008**, *345*, 275–282.
(23) Cottone, G.; Cordone, L.; Ciccotti, G. *Biophys. J.* **2001**, *80*, 931–938.
(24) Cottone, G. *J. Phys. Chem. B* **2007**, *111*, 3563–3569.
(25) Giuffrida, S.; Cottone, G.; Librizzi, F.; Cordone, L. *J. Phys. Chem. B* **2003**, *107*, 13211–13217.
(26) Giuffrida, S.; Cottone, G.; Cordone, L. *Biophys. J.* **2006**, *91*, 968–980.
(27) Cordone, L.; Cottone, G.; Giuffrida, S.; Palazzo, G.; Venturoli, G.; Viappiani, C. *Biochim. Biophys. Acta, Proteins Proteomics* **2005** *1749*, 252−281 (and references therein).
(28) Cordone, L.; Cottone, G.; Giuffrida, S. *J. Phys.: Condens. Matter* **2007** *19*, 205110 (and references therein).
(29) Francia, F.; Dezi, M.; Mallardi, A.; Palazzo, G.; Cordone, L.; Venturoli, G. *J. Am. Chem. Soc.* **2008**, *130*, 10240–10246.
(30) Longo, A.; Giuffrida, S.; Cottone, G.; Cordone, L. *Phys. Chem. Chem. Phys.* **2010**, *12*, 6852–6858.
(31) Bellavia, G.; Cordone, L.; Cupane, A. *J. Therm. Anal. Calorim.* **2009**, *95*, 699–702.
(32) Cammarata, M.; Levantino, M.; Wulff, M.; Cupane, A. *J. Mol. Biol.* **2010**, *400*, 951–962.
(33) Sasanuma, K.; Seshimo, Y.; Hashimoto, E.; Ike, Y.; Kojima, S. *Jpn. J. Appl. Phys.* **2008**, *47*, 3843–3846.
(34) Roos, Y. *J. Therm. Anal. Calorim.* **1997**, *48*, 535–544.
(35) Hayashi, Y.; Puzenko, A.; Balin, I.; Ryabov, Y. E.; Feldman, Y. *J. Phys. Chem. B* **2005**, *109*, 9174–9177.
(36) Gordon, M.; Taylor, J. S. *J. Appl. Chem.* **1952**, *2*, 493–500.
(37) Voss, N. R.; Gerstein, M. *J. Mol. Biol.* **2005**, *346*, 477–492.
(38) Bordat, P.; Lerbret, A.; Demaret, J.-P.; Affouard, F.; Descamps, M. *Europhys. Lett.* **2004**, *65*, 41–47.
(39) Sussich, F.; Cesàro, A. *J. Therm. Anal. Calorim.* **2000**, *62*, 757–768.
(40) Hallbruker, A.; Mayer, E.; Johari, G. P. *J. Phys. Chem.* **1989**, *93*, 4986–4990.
(41) Velikov, V.; Borick, S.; Angell, C. A. *Science* **2001**, *294*, 2335–2338.
(42) Lee, A. L.; Wand, A. J. *Nature* **2001**, *411*, 501–504.
(43) Doster, W.; Cusack, S.; Petry, W. *Nature* **1989**, *337*, 754–756.
(44) Bajaj, V. S.; van der Wel, P. C. A.; Griffin, R. G. *J. Am. Chem. Soc.* **2009**, *131*, 118–128.
(45) Schirò, G.; Sclafani, M.; Caronna, C.; Natali, F.; Plazanet, M.; Cupane, A. *Chem. Phys.* **2008**, *345*, 259–266.
(46) Schirò, G.; Sclafani, M.; Caronna, C.; Natali, F.; Plazanet, M.; Cupane, A. *Eur. Biophys. J.* **2008**, *37*, 543–549.
(47) Schirò, G.; Caronna, C.; Natali, F.; Cupane, A. *J. Am. Chem. Soc.* **2010**, *132*, 1371–1376.
(48) Schirò, G.; Caronna, C.; Natali, F.; Cupane, A. *Phys. Chem. Chem. Phys.* **2010**, *12*, 10215–10220.
(49) Slade, L.; Levine, H. *Adv. Food Nutr. Res.* **1995**, *38*, 103–269.
(50) Giuffrida, S.; Troia, R.; Schiraldi, C.; D'Agostino, A.; De Rosa, M.; Cordone, L. *Food Biophys.* [Online early access]. DOI: 10.1007/s11483-010-9197-5. Published Online: Dec 22, 2010.